7-2001

The Expansion Center and Dynamical Age of the Galactic Supernova Remnant Cassiopeia A

John R. Thorstensen
Dartmouth College

Robert A. Fesen
Dartmouth College

Sidney van den Bergh
National Research Council of Canada

THE ASTRONOMICAL JOURNAL, 122:297–307, 2001 July

THE EXPANSION CENTER AND DYNAMICAL AGE OF THE GALACTIC SUPERNOVA REMNANT CASSIOPEIA A[1]

JOHN R. THORSTENSEN AND ROBERT A. FESEN
Department of Physics and Astronomy, 6127 Wilder Laboratory, Dartmouth College, Hanover, NH 03755

AND

SIDNEY VAN DEN BERGH
Dominion Astrophysical Observatory, Herzberg Institute of Astrophysics, National Research Council of Canada, 5071 West Saanich Road, Victoria, BC V9E 2E7, Canada
Received 2001 February 25; accepted 2001 April 10

ABSTRACT

We present proper motions for 21 bright main shell and 17 faint, higher velocity, outer ejecta knots in the Cas A supernova remnant and use them to derive new estimates for the remnant's expansion center and age. Our study included 1951–1976 Palomar 5 m prime focus plates, 1988–1999 CCD images from the KPNO 4 m and MDM 2.4 m telescopes, and 1999 *HST* WFPC2 images. Measurable positions covered a 23 to 41 yr time span for most knots, with a few outer knots followed for almost 48 yr. We derive an expansion center of α(J2000) = $23^h23^m27^s.77 \pm 0^s.05$, δ(J2000) = $58°48'49''.4 \pm 0''.4$ (ICRS), with little difference between centers derived using outer or main shell knots. This position is $3''.0$ due north of that estimated by van den Bergh & Kamper. It also lies $6''.6 \pm 1''.5$ almost due north (P.A. = 354°) of the remnant's recently detected central X-ray point source, implying a transverse velocity for the X-ray point source $\simeq$330 km s^{-1} at a distance of 3.4 kpc. Using the knots which lie out ahead of the remnant's forward blast wave, we estimate a knot convergent date of A.D. 1671.3 ± 0.9 assuming no deceleration. However, a deceleration of just $\sim$1.6 km s^{-1} yr^{-1} over a 300 yr time span would produce an explosion date $\simeq$A.D. 1680, consistent with the suspected sighting of the Cas A supernova by J. Flamsteed.

Key words: ISM: individual (Cassiopeia A) — ISM: kinematics and dynamics — supernova remnants

1. INTRODUCTION

Cassiopeia A (Cas A) is the youngest Galactic supernova remnant (SNR) known and, with the exception of the Sun, ranks as the strongest discrete radio source in the sky at 100–1000 MHz. At radio, optical, and X-ray wavelengths, Cas A consists of a $\simeq 2'$ radius broken shell of SN debris rich in O, S, Si, Ar, Ca expanding at 4000–6000 km s^{-1}. Within this shell lie about two dozen knots of much slower moving, N-rich clumps of pre-SN, circumstellar mass loss material. Outside of the shell, faint radio and X-ray emission extends to a radial distance of $\simeq 160''$, where a faint, filamentary edge of X-ray emission marks the current location of the remnant's forward shock front. At an estimated distance of $3.4^{+0.3}_{-0.1}$ kpc (Reed et al. 1995), these angular dimensions correspond to main shell and outer shock front radii of 2 and 2.7 pc, respectively. Several dozen faint optical knots with velocities of 8000 to 15,000 km s^{-1} have been detected outside some sections of the main shell, mainly in a northeastern "jet" of high speed ejecta (Fesen & Gunderson 1996; Fesen 2001).

The remnant's precise age is uncertain. From proper motion studies for $\sim$100 of Cas A's optical knots during 1951–1980, Kamper & van den Bergh (1976, hereafter KvdB76) and van den Bergh & Kamper (1983, hereafter vdBK83) determined an explosion date of 1658 ± 3 for the remnant as a whole (assuming no deceleration) and a somewhat later date of 1671 for a few higher-velocity northeastern "jet" knots. The difference between these derived dates probably reflects a greater deceleration of bright main shell knots caused by their interaction with the remnant's reverse shock.

There are no unambiguous historical observations of a bright nova or variable star in Cassiopeia that might be associated with a late 17th century supernova. However, on 1680 August 16 John Flamsteed, the first Astronomer Royal, reported seeing a 5th–6th magnitude star he designated "supra τ" and later renamed 3 Cassiopeiae in his 1725 Historia Coelestia star catalog (Ashworth 1980). Its proximity to Cas A, together with the fact that he never observed this star again, raises the possibility that he sighted the Cas A supernova in the summer of 1680.

The positional differences between Cas A and the 3 Cas position are, however, troublingly large. Flamsteed's location for 3 Cas is offset from Cas A by $12'.1$ in right ascension and $8'.6$ in declination. Although refraction and sextant corrections might decrease these residuals to $\simeq 6'$ in both coordinates (errors not unprecedented for Flamsteed), the case for Flamsteed's sighting of Cas A is controversial (Broughton 1979; Kamper 1980; Hughes 1980).

Without additional evidence, the significance of Flamsteed's observation might well remain inconclusive. However, the large proper motions of the remnant's ejecta knots ($\mu = 0''.4$–$0''.6$ yr^{-1}) can be used to set limits on Cas A's age and thereby test the possible 1680 explosion date. An accurate measurement of Cas A's age would in turn provide key information about deceleration of its high-speed knots and thus the phase of its evolutionary development.

Accurate proper motion measurements can also be used to improve determinations of the remnant's center of expansion. KvdB76 determined the remnant's expansion center to within an error radius of about $1''$. No optical point source

[1] Based in part on observations with the NASA/ESA *Hubble Space Telescope*, obtained at the Space Telescope Science Institute, which is operated by the Association of Universities for Research in Astronomy, Inc., under NASA contract NAS 5-26555.

or extended emission is present at this location down to $I \sim 24$ mag (van den Bergh & Pritchet 1986).

Knowledge of Cas A's precise expansion center has recently gained greater interest with the *Chandra X-Ray Observatory* discovery of an X-ray point source near the remnant's center (Tananbaum 1999). This object, which could be either a neutron star with magnetized polar caps or an accreting compact object (Pavlov et al. 2000; Umeda et al. 2000; Chakrabarty et al. 2001), lies significantly offset from estimates for the remnant's center of expansion (COE). Point source coordinates derived from *ROSAT* and *Chandra* data show a separation of 1″–5″ from the KvdB76 and vdBK83 COE, and some 16″–20″ from the COE inferred by Reed et al. (1995) using knot radial velocities. These offsets imply transverse velocities of 50–250 km s^{-1} and 800–1000 km s^{-1}, respectively, assuming $d = 3.4$ kpc and an age of 320 yr (Pavlov et al. 2000).

In this paper, we present proper motions of 17 outlying high-velocity ejecta knots discovered over the last decade (see Fesen 2001 and references therein) along with 21 selected main shell knots. Many of these 40 knots can be seen on the earliest archival Palomar 5 m PF plates, giving proper motion baselines of nearly five decades, or about 1/7th of the remnant's age. We use these proper motions to determine a more accurate position and date for the supernova.

2. EJECTA KNOT OBSERVATIONS

2.1. *Image Data*

Our observational material includes Palomar 5 m prime focus (PF) plates dating back to 1951, CCD images taken 1988–1999 with the KPNO 4 m and MDM 2.4 m telescopes, and a few 1999 *HST* WFPC2 images. Table 1 lists information on the images that were used. Although archival plates and modern CCD image data have, in many cases, substantially different spectral sensitivities, the angular scale of knot emission stratification or ionization structures lies well below all but the highest resolution *HST* data (Fesen et al. 2002, in preparation) and thus does not pose a significant problem for the intercomparison of knot positions from these different data sets.

To maximize the time base, we examined several dozen archival Palomar 5 m PF plates beginning with R. Minkowski in 1951 and ending with S. van den Bergh in 1989. Most of these plates were unsuitable for this project because of poor image quality or weak knot detection, but four were selected for use. These included two plates taken on back-to-back nights in 1951, a better and deeper 1958 image (van den Bergh & Dodd 1970, their Fig. 1), and a superb 1976 image (vdBK83).

Modern CCD interference and broadband filter images of all or portions of the Cas A remnant obtained from 1988 November through 1999 October were also measured. Several of these have been used in prior studies, and a few were taken expressly for this project. Some high resolution 1999 epoch WFPC2 *HST* images were also used for several outlying northern and jet knots.

We selected for measurement a total of 38 ejecta knots that had measurable positions on the Palomar 1976 and later images ($\Delta t = 23$ yr). Many were outer knots, together with some shell knots visible from 1958 through 1999 ($\Delta t = 41$ yr). Nearly a dozen knots, mostly among the outer ejecta, were detectable from 1951 through 1999, a span of almost 48 years, which is about 15% of Cas A's age.

It is unlikely that suitable earlier images exist. The Palomar 5 m was completed in 1948, coincident with the discovery of Cas A as a localized radio source (Ryle & Smith 1948). Furthermore, the remnant has brightened significantly over the last half-century (van den Bergh & Kamper 1985), and the individual knots often have finite visibility lifetimes (KvdB76). These factors set a practical limit of ~ 50 yr for the time span over which the proper motion can be studied at this time.

2.2. *Knot Selection*

Of the 38 knots selected, 21 were main shell features and 17 were outer, higher velocity knots in the NE jet or elsewhere. Figure 1 shows the location of the selected knots. Table 2 cross-lists our designations with those of earlier studies where possible.

Our two main knot selection criteria were as follows. (1) *Distinct appearance with an absence of significant morpho-*

TABLE 1

OBSERVATIONAL MATERIAL USED FOR PROPER MOTIONS

Date (UT)	Telescope	Plate No./Image ID	Scale (arcsec $pixel^{-1}$)	Emulsion/Bandpass	Region Imaged	Exposures (s)
1951 Nov 01.....	Palomar 5 m	553B	0.1406	103aE + RG2	Whole SNR	1 × 7200
1951 Nov 02.....	Palomar 5 m	563B	0.1406	103aE + RG2	Whole SNR	1 × 7200
1958 Aug 11.....	Palomar 5 m	3033S	0.1406	103aF + RG2	Whole SNR	1 × 5400
1976 Jul 02	Palomar 5 m	7252vB	0.1406	098-04 + RG645	Whole SNR	1 × 7200
1988 Nov 10.....	KPNO 4 m	...	0.297	[S II] λ6725	Jet, east limb	5 × 128
1988 Nov 10.....	KPNO 4 m	...	0.297	Hα + [N II]	Jet, east limb	5 × 192
1992 Jul 05	MDM 1.3 m	...	0.635	Broad [S II] λ6725	Whole SNR	3 × 1800
1992 Jul 05	MDM 1.3 m	...	0.635	Hα + [N II]	Whole SNR	3 × 1800
1996 Oct 06	MDM 2.4 m	...	0.275	Broad [S II] λ6725	NW, SW, NE, SE	2 × 1000
1996 Oct 07	MDM 2.4 m	...	0.275	Hα + [N II]	NW, SW, NE, SE	2 × 600
1996 Oct 07	MDM 2.4 m	...	0.275	Cont. 6450 Å	NW, SW, NE	2 × 1000
1999 Jun 12	*HST* 2.4 m	U52B0194R–0109R	0.0996	[S II] (F673N)	Jet	6 × 1000
1999 Jun 12	*HST* 2.4 m	U52B010CR–010FR	0.0996	*R* (F675W)	Jet	4 × 600
1999 Jun 13	*HST* 2.4 m	U52B0205R–0207R	0.0996	R (F675W)	NW limb	3 × 500
1999 Jun 13	*HST* 2.4 m	U52B0205R–020BR	0.0996	*R* (F675W)	West limb	2 × 700
1999 Oct 15	MDM 2.4 m	...	0.275	*R*	Whole SNR	2 × 720

NOTE.—Original Palomar 5 m plate scale: 11.″1 mm^{-1}.

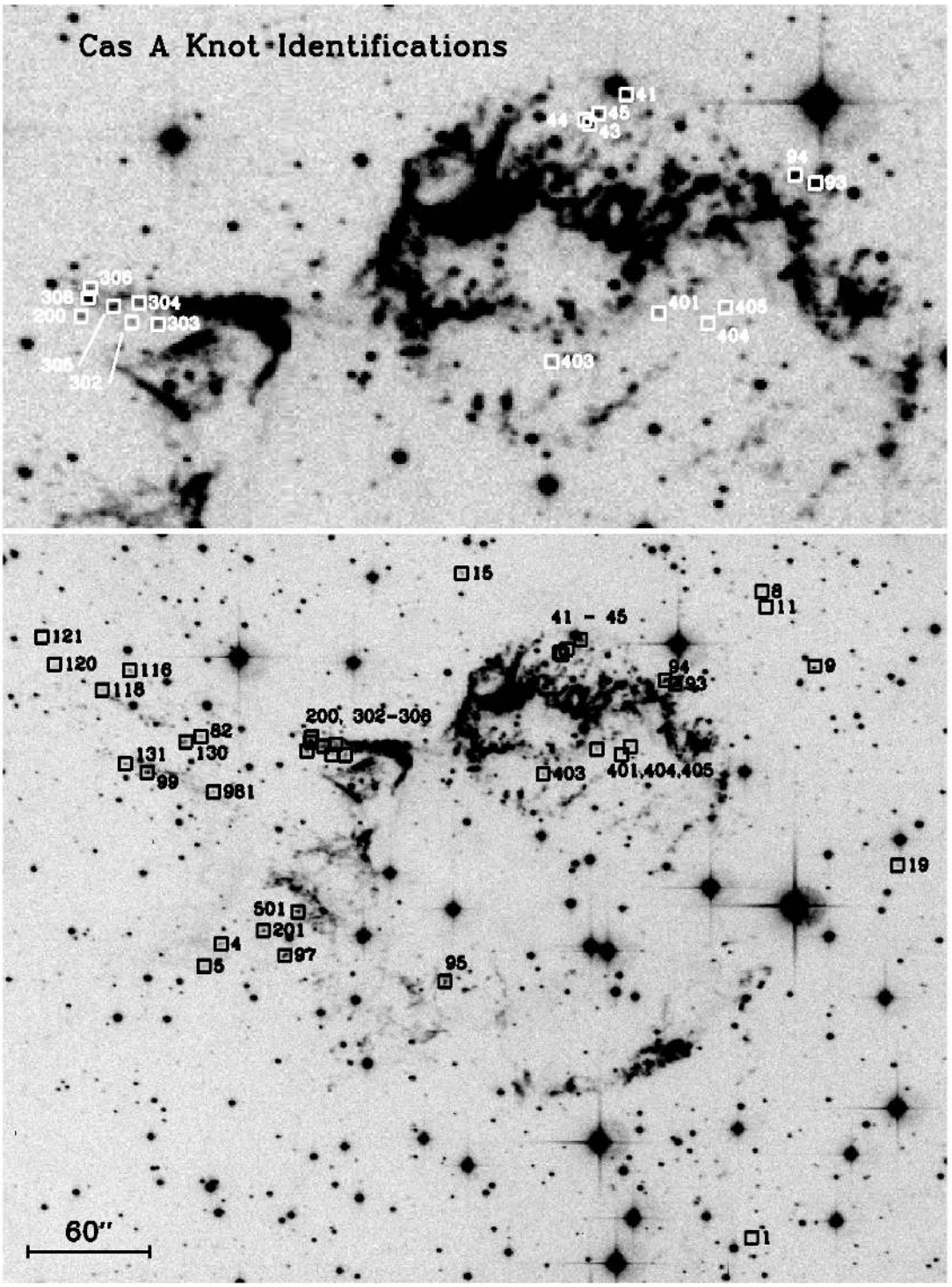

FIG. 1.—[S II] λλ6716, 6731 image of Cas A from 1992 July (Fesen & Gunderson 1996). The lower panel shows all the knots used in this study. The upper panel is a magnified view of the main shell region. The positions marked are derived from the knot trajectories adjusted to the epoch of the image. Some of the knots are not visible.

logical changes. We looked for knots which were compact with steady morphologies that allowed secure identification and centroiding. None of the knots was perfect, but some, like the bright outer knot 15, provided excellent positional measurements over the entire 48 yr time span surveyed. Like most other outlying fast-moving knots, it has a relatively stable morphology (see Fesen 2001). On the other hand, main shell knots can show substantial changes in appearance on images separated by just 5 to 10 yr. Consequently, we included only the most distinct and persistent main-shell features. The number of main-shell features we used was therefore relatively small compared to prior studies (KvdB76 and vdBK83). (2) *Time span of visibility*. The longer a knot is measurable, the greater weight it has for determining the remnant's expansion center. We therefore biased our knot selection toward knots with long visibility time spans ($\geq$20 yr). This resulted in a much smaller knot sample than the 102 measured by KvdB76. Their

TABLE 2

PROPER MOTION KNOT IDENTIFICATION (ID) REFERENCES

Knot IDs	Prior IDs for Knots	Reference
	Outer Knots	
1, 4, 5, 8, 9	1, 4, 5, 8, 9	FBB87, FBG88
11	11	FBG88
15	KB91, 15	vdBK83; FBB87; FBG88
19	19	Fesen 2001
	Knots in NE Jet	
82	82	FB91
99	115	vdBK83; FBG88
116.....	116	KvB76, vdBK83; FBG88
118, 120, 121.....	118, 120, 121	FBG88
130.....	113	vdBK83
131.....	...	This paper
	Shell Knots	
93	41	KvdB76, vdBK83
94	7	KvdB76, vdBK83
95	...	this paper
97	111	vdBK83
200.....	...	this paper
201.....	...	this paper
302.....	102	KvdB76, vdBK83
303.....	...	this paper
304.....	101	KvdB76, vdBK83
305.....	105	KvdB76, vdBK83
306.....	...	this paper
308.....	...	this paper
401.....	...	this paper
403.....	65	KvdB76
404.....	...	this paper
405.....	...	this paper
41	59	KvdB76
43	14	KvdB76, vdBK83
44	...	this paper
45	63	KvdB76
501.....	1 ?	KvdB76
981.....	...	this paper

REFERENCES.—(FB91) Fesen & Becker 1991; (FBG88) Fesen, Becker, & Goodrich 1988; (FBB87) Fesen, Becker, & Blair 1987; (KvdB76) Kamper & van den Bergh 1976; (vdBK83) van den Bergh & Kamper 1983.

knots covered time spans ranging from 3 to 24 yr, with 46% of their knots visible for less than 15 yr.

3. ASTROMETRIC PROCEDURES AND MEASUREMENTS

3.1. *Reference Star Grid*

We began by constructing a grid of reference stars. First, centroids for several hundred unsaturated stars were measured on the Hα and [S II] λλ6716, 6731 images taken with the MDM 1.3 m telescope in 1992 July, using the IRAF incarnation of DAOPHOT (Stetson 1987). We then cross-identified these stars with the USNO A2.0 catalog (Monet et al. 1996) and derived a six-constant linear plate model, rejecting stars with large residuals. Because the centroids in the CCD data have much better internal precision than the USNO A2.0 coordinates, we transformed the CCD centroids to right ascension and declination using the plate model and averaged the results from the Hα and [S II] exposures. This procedure yielded right ascensions and declinations approximately on the International Coordinate Reference System (ICRS) of the USNO A2.0, but with much higher internal precision. The USNO A2.0 is based on the original Palomar Observatory Sky Survey plates, which for this field are epoch 1954.6, so the elimination of high-residual stars removes stars with appreciable proper motions, as well as blended images and other difficult cases. For the final step, the refined celestial coordinates were converted to tangent-plane coordinates, using the KvdB76 center of expansion as the tangent point. The final reference grid consisted of 141 stars with red magnitudes (from the USNO A2.0) from 15.2 to 19.1 covering an $8' \times 8'$ field.

Because this reference star grid is fundamental to all our results, we checked it for various sources of error: (1) errors in the grid's *coordinate zero point* which would affect comparisons with other results, (2) *proper motion* of the grid stars, and (3) *radial distortions* in the grid which could cause a systematic error in the age estimate. Below, we consider each of these sources of error in turn.

3.1.1. *Zero Point for Reference Grid*

We performed two checks on the positional zero point of the reference star grid.

First, we examined the twelve reference stars (for epoch 1965) tabulated by KvdB76. We measured these stars on all the images on which they appeared, used our reference star net to derive positions and proper motion as described below for the knots, and compared the results to those tabulated in KvdB76. Ten of the 12 KvdB76 reference stars had sufficient observations in our data. For these, our right ascensions were on average 485 mas larger than theirs, with an rms scatter of 67 mas, while our declinations were 448 mas smaller, with a scatter of 112 mas.

Second, during the preparation of this work, the Tycho-2 astrometric catalog became available (Høg et al. 2000). Four Tycho-2 stars appear on enough images to derive good positions for epoch J2000, and for three stars the time base gives adequate proper motions. Because the stars were highly saturated in nearly all our pictures, we estimated the star' centers and their uncertainties by eye. Our derived epoch 2000 positions for the four Tycho stars are, on average 121 ± 80 mas east and 82 ± 79 mas south of the catalog positions, well within the accuracy to which the USNO A2.0 is expected to align with the ICRS.

The Tycho and USNO catalogs are based on *Hipparcos* observations, which should provide much more reliable all-sky positions than the catalogs available to KvdB76. We conclude that our grid is in registration with the ICRS to within $\pm 0\farcs2$ at worst and that KvdB may have suffered a barely significant zero-point error.

3.1.2. *Proper Motions of Grid Stars*

In deriving plate models, we did not adjust the positions of our grid stars for proper motions. We implicitly assumed that the proper motions of the grid stars were small. Our grid stars are on average only a little brighter than the dozen $V \sim 19$ mag reference stars used by KvdB76. They remark that stars this faint should have intrinsic proper motions from the solar motion and Galactic rotation of ~ 1 mas yr^{-1}. It is therefore likely that our grid stars' motions are similarly small. A systematic offset $\mu_{\rm sys}$ in proper motions can seriously affect the derived center for the SNR, since it displaces the center by $\mu_{\rm sys} \times \sim 300$ yr.

For the three Tycho-2 stars for which proper motions could be derived on our reference grid, the weighted averages of $\mu_{\rm T2} - \mu_{\rm grid}$ were -3.5 ± 2.5 mas yr^{-1} in right ascen-

sion and $+0.8 \pm 2.5$ mas yr^{-1} in declination. Therefore, there was no evidence for a significant motion with respect to the ICRS.

The comparison with the KvdB reference stars was a bit more complex. They explicitly derived proper motions for their reference stars and found a 9 mas yr^{-1} mean proper motion in declination. They decided this was spurious and later adjusted their derived Cas A center to account for the drift in their reference grid. Reducing 10 of their reference stars with respect to our grid gives mean differences $\mu_{\rm KV} - \mu_{\rm ref}$ of -2.8 ± 1.4 mas yr^{-1} in right ascension and $+8.3 \pm 1.4$ mas yr^{-1} in declination. This is just as expected on the basis of their remarks. Indeed, our procedure is logically similar to theirs, but less complex: we simply assumed the faint grid to be motionless ab initio, while they derived proper motions and corrected them at the end to achieve the same result.

Finally, we checked our grid stars individually against the reference grid, deriving proper motions for each star based on all the images on which it appeared. Formally, this was flawed by the inclusion of the star itself in the plate models, but with our sample of 140 stars, the effect should be negligible. Grid stars observed over the whole range of dates had typical estimated proper motion uncertainties of $\pm \sim 1.7$ mas yr^{-1}, and relatively few showed significant proper motions. In the fitting procedure used for the images (described below), grid stars with large residuals were iteratively clipped out, so the few stars with significant proper motions did not affect our results.

From all these tests, we conservatively estimate the grid to be inertial to within ~ 2 mas yr^{-1}.

3.1.3. *Field Distortions*

The procedure used to set up the reference grid is valid provided that distortions in the field of the MDM 1.3 m telescope are insignificant. This is likely to be the case. Cudworth & Rees (1991) measured the field distortions of several southern telescopes, including the CTIO 1.5 m which, like the MDM 1.3 m, is an f/7.5 Ritchey-Chretien reflector. If one equipped the CTIO 1.5 m with a CCD having the same size as that used in deriving our reference grid, then their radial distortion term a_9 would contribute only 7 mas at the corners of the field of view.

Nonetheless, we searched for field distortions in several different ways. (1) In fitting the USNO A2.0 stars, we did not see any trends in the residuals from the six-constant plate model. The USNO A2.0 typically has centroiding errors in the 250–500 mas range. In view of the number of stars used, this alone limits systematic trends to ≤ 200 mas. (2) We examined archival CCD images of the globular cluster M13 taken with the MDM 1.3 m and the same camera as the Cas A images. Kyle Cudworth kindly provided us with a list of star positions in M13, which he estimated were accurate to ~ 20 mas for relative positions. A six-constant fit of the CCD centroids to those positions gave an rms residual of 70 mas, again showing no obvious systematic trends. When a more elaborate model was used, the residuals were not improved significantly. The scatter is somewhat larger than expected but does not seem to indicate any field distortions. (3) In 1999 October we obtained a set of short I-band CCD exposures of Cas A with the MDM 2.4 m telescope, covering an $8' \times 8'$ field. A six-constant fit to the 124 standard reference stars included in this image gave an rms residual of 60 mas, without any iteration; iterative clipping of high residuals brought this down to 34 mas, with 110 stars remaining. Again, a more elaborate fit did not result in significant improvement.

Because the reference grid is based on exposures taken with the MDM 1.3 m, this last test simply compares the two telescopes. However, in 2000 January we also performed an astrometric calibration of the 2.4 m by obtaining two sets of short-exposure 2.4 m images of a portion of the Stone, Pier, & Monet (1999) astrometric standard region E. In one set of images, we fitted 172 stars to a six-constant plate model. This gave a 153 mas rms residual. Iterative elimination of the largest residuals brought this down to 53 mas with 114 stars. Similar results were found with the other set of images. The residual maps of the two sets of images did not show systematic distortions but were highly correlated with each other. This suggests that most of the error arises from the catalog positions, probably due to the (necessary) inclusion of many stars near the faint limit of the catalog.

In summary, the tests we made did not show any geometric distortion in our reference grid. The results suggest that systematic distortions are smaller than ~ 60 mas and that the centering precision of the reference stars is conservatively ~ 50 mas.

3.2. *Image Solutions*

We scanned the four Palomar PF plates (Table 1) on the Yale Astronomy Department's PDS microdensitometer. We used a 13.3 μm $\times$ 13.3 μm scanning aperture and sampled every 12.656 μm in a 3300 $\times$ 4100 raster centered on the remnant, the long dimension being east-west. The plate scale was $11''.1$ mm^{-1}, yielding $0''.141$ pixel^{-1}. We used SExtractor (Bertin & Arnouts 1996) to derive star centers for the Palomar plates.

The Palomar 5 m prime-focus camera used a corrector which produced substantial radial distortions. Similar corrector distortions have been discussed by Murray (1971) and Cudworth & Rees (1991). Plate coordinates of the distortion center, (x_0, y_0), enter the least-squares models in a nonlinear fashion, so following Murray (1971) and Cudworth & Rees (1991) we estimated (x_0, y_0) in a separate step. We first fitted the reference stars with a simple six-constant plate model of the form

$$X_0 = a_0 + a_1 x + a_2 y ,$$

where X_0 is the standard reference star coordinate, and x and y are the coordinates on the Palomar plate. This fit gave root mean square (rms) residuals of ~ 240 mas, with maximum values ~ 690 mas. The distortion center (x_0, y_0) could then easily be estimated from the residual maps. These were then used in a 16-constant model of the form

$$X_0 = a_0 + a_1 x + a_2 y + a_3 x^2 + a_4 xy + a_5 y^2 + a_6 xr^2 + a_7 xr^4 ,$$

where $r^2 = [(x - x_0)^2 + (y - y_0)^2]^{1/2}$. This model is similar to that used by Cudworth & Rees (1991), but without magnitude terms. As expected, these fits were much better; after a few of the highest-residual stars were rejected, rms residuals ranged from 71 mas (P7252) to 133 mas (P553B).

Fitting the CCD images was more straightforward. We centroided the reference stars with DAOFIND and matched them to their standard star XY coordinates. For the ground-based CCD images, there were always more than 20 stars matched. Because distortions in the CCD

TABLE 3

KNOT POSITIONS AND PROPER MOTIONS

Knot ID	α	δ	μ_α (mas yr^{-1})	μ_δ (mas yr^{-1})	σ_x (mas)	σ_μ (mas yr^{-1})	First Epoch	Last Epoch
1	23 23 12.943	58 45 57.97	−341	−509	113	10	1958.61	1996.77
4	23 23 47.327	58 48 26.40	454	−70	172	9	1951.83	1996.76
5	23 23 48.455	58 48 15.05	488	−108	83	5	1951.83	1999.79
8	23 23 12.202	58 51 24.06	−370	467	74	5	1951.83	1999.79
9	23 23 08.738	58 50 46.53	−458	362	69	4	1951.83	1999.79
11	23 23 11.921	58 51 16.43	−391	454	143	15	1976.50	1999.45
15	23 23 31.727	58 51 33.51	97	500	77	4	1951.83	1999.79
19	23 23 03.424	58 49 05.79	−571	49	58	6	1976.50	1999.79
41	23 23 23.993	58 50 59.85	−92	380	181	12	1958.61	1999.79
43	23 23 25.187	58 50 52.39	−67	365	152	9	1951.83	1999.79
44	23 23 25.367	58 50 53.47	−44	376	148	10	1958.61	1999.79
45	23 23 24.891	58 50 55.07	−71	369	150	9	1958.61	1999.79
82	23 23 48.677	58 50 11.11	491	252	72	8	1976.50	1999.79
93	23 23 17.839	58 50 37.52	−222	331	114	6	1951.83	1999.79
94	23 23 18.480	58 50 39.43	−225	327	97	5	1951.83	1999.79
95	23 23 32.801	58 48 07.52	110	−111	76	10	1958.61	1999.79
97	23 23 43.194	58 48 20.64	345	−77	115	6	1958.61	1999.79
99	23 23 52.171	58 49 53.03	580	194	48	6	1958.61	1999.79
116	23 23 53.316	58 50 44.52	604	358	78	6	1951.83	1999.79
118	23 23 55.062	58 50 34.58	616	322	89	11	1976.50	1999.79
120	23 23 58.184	58 50 47.51	719	360	107	10	1976.50	1999.79
121	23 23 59.032	58 51 01.44	730	411	107	13	1958.61	1996.76
130	23 23 49.665	58 50 08.48	508	242	141	9	1958.61	1999.79
131	23 23 53.600	58 49 57.28	607	203	195	21	1976.50	1996.76
200	23 23 41.778	58 50 03.71	321	215	69	10	1976.50	1999.79
201	23 23 44.598	58 48 33.20	381	−46	60	6	1958.61	1999.79
302	23 23 40.139	58 50 02.10	287	212	126	8	1958.61	1999.79
303	23 23 39.275	58 50 01.73	260	205	157	10	1958.61	1996.76
304	23 23 39.899	58 50 07.15	285	233	141	9	1958.61	1999.79
305	23 23 40.732	58 50 06.15	307	225	162	10	1958.61	1999.79
306	23 23 41.484	58 50 10.88	324	247	143	10	1958.61	1999.79
308	23 23 41.525	58 50 08.33	307	222	170	18	1976.50	1999.79
401	23 23 22.948	58 50 04.47	−108	219	124	8	1951.83	1999.79
403	23 23 26.438	58 49 52.17	−22	188	140	10	1951.83	1999.79
404	23 23 21.358	58 50 01.91	−142	217	136	8	1958.61	1999.79
405	23 23 20.757	58 50 05.96	−172	232	158	11	1958.61	1999.79
501	23 23 42.343	58 48 42.61	329	−16	157	14	1976.50	1999.79
981	23 23 47.840	58 49 43.04	470	168	120	11	1951.83	1976.50

NOTES.—Positions are for epoch J2000 and are referred to the ICRS. Units of right ascension are hours, minutes, and seconds, and units of declination are degrees, arcminutes, and arcseconds.

images were expected to be relatively small, we used the six-constant model described above, with any unruly stars omitted by iterative clipping.

Reduction of the few *HST* images was not as simple. First, the images from the four CCDs of the WFPC2 were interpolated onto a single grid using the "wmosaic" task in the IRAF STSDAS package, which approximately corrects for field distortions. Unfortunately, the WFPC2 field of view is so small that one of our fields had only six reference stars. To increase the number of reference stars we measured some fainter stars on the "wide [S II]" 2.4 m image from 1999 October, transformed these over to the standard grid and used them in the fit to the *HST* data. With these added stars, each *HST* field had at least 14 reference stars. The rms scatter for the six-constant models was 50 to 55 mas. Holtzman et al. (1995) quote an rms scatter of 10 mas in their fit to the WFPC2 field distortions. The larger scatter found here probably arises from the errors in the reference star positions. In particular, there was no pattern indicating that the zero-point offsets between the CCDs were different from those assumed by wmosaic.

3.3. *Knot Measurements and Fits*

We tried several methods to measure positions of the selected 38 knots. This was a somewhat complicated problem, since many of the knots were resolved in our images. The dominant source of centering uncertainty resulted from structure in the knots, rather than photon or grain noise. In the end, we simply estimated the knot centers by eye using a cursor on an image display. We allowed our judgment to be informed by centroids from such tools as the "imexamine" task in IRAF and (for the photographic scans) the centers from SExtractor. The selected knots often had "head-tail" structures, in which case we estimated the center of the head. Some of the shell knots were embedded in nebulosity. In such cases, we tried to center on the brightest part of the knot.

Our uncertainty estimates were also subjective, but we attempted to err on the conservative side. When we later fitted straight-line trajectories to the knots, we found that the residuals were often smaller than one would expect on the basis of our estimated uncertainties, demonstrating that

our estimates were indeed conservative. For the photographic images, our estimated errors were guided by lower bounds on the error based on the noise in the plate fog, the central brightness of the knot, and the knot's angular size. These bounds were calibrated with a Monte Carlo simulation.

Once xy coordinates were measured on all the images, they were transformed to the tangent-plane coordinate system using the solutions described earlier. The rms scatter in the plate solution was added in quadrature to each the knot's estimated uncertainty. If the rms scatter was less than 40 mas, it was set to 40 mas to account for systematics. Transformed knot positions were automatically collated with the exposure epochs for the images, yielding a time series of positions for each knot.

Finally, each knot's trajectory was fitted with a straight line,

$$X(t) = X_0(t_0) + \mu_X(t - t_0) ,$$

where t_0 is the weighted mean epoch of observation, and similarly for Y. Uncertainties were propagated into the coefficients in a standard manner. Table 3 gives the results of this procedure.

4. RESULTS AND DISCUSSION

4.1. *Cas A's Center of Expansion*

Figure 2*a* shows the trajectories of our selected knots extrapolated back to A.D. 1600, somewhat before the estimated explosion date. The dots are the individual knot measurements with the width of each line indicating its statistical weight.

Because the knots may have decelerated by varying amounts, we estimated the center using only the knots' lines of position and did not apply any constraints arising from the time dependence (i.e., forcing the knots to start at the same epoch). We constructed a trajectory for each knot and computed its positional uncertainty σ_{i0} near the time of the explosion by propagating the estimated position and proper motion errors. Because of the long time lever, the proper motion uncertainty dominated the errors in all cases. With this information we could compute, for any X and Y, a likelihood function of the form

$$\lambda(X, Y) = \prod_i \frac{1}{2\sigma_{i0}} \exp\left(-d_{i\perp}^2/2\sigma_{i0}^2\right) ,$$

where $d_{i\perp}$ is the perpendicular distance between (X, Y) and the knot's line of position. The (X, Y) which maximizes this is our estimate of the expansion center.

This procedure gave $X = +91$ mas and $Y = +2812$ mas, referred to the KvdB76 center. This translates into α(J2000) = $23^h23^m27^s.77 \pm 0^s.05$, δ(J2000) = $58°48'49''.4 \pm 0''.4$. The center derived using only the outer knots nearly coincided with that derived from the selected shell knots. Table 4 lists our main shell and outer knot centroids separately along with our final values for the whole sample. The errors given are purely statistical, based on the Monte Carlo calibration of the centering errors (see below).

4.1.1. *Error Estimates*

Because our expansion center differs from those of previous estimates (see below), we estimated our measurement uncertainties in several ways.

Since we have computed a likelihood function, the likelihood-ratio test described by Cash (1979) can be used to form confidence contours. Such contours, however, assume that the positional errors we estimated by eye are truly one standard deviation. The resulting 95% confidence contour is an oval slightly elongated northwest-southeast, with a radius $\sim 1''.3$. Figure 3 is a magnified view of the center region, showing the lines of position together with the 95% to 99.5% confidence contours from this procedure.

We also used a Monte Carlo simulation of the proper motion measurements to check our uncertainties and to normalize our error estimates. We began by assuming that the explosion occurred at the observed maximum-likelihood position. Then, taking each knot's present position as known and fixed (because the proper motions dominate the errors), we computed an idealized proper

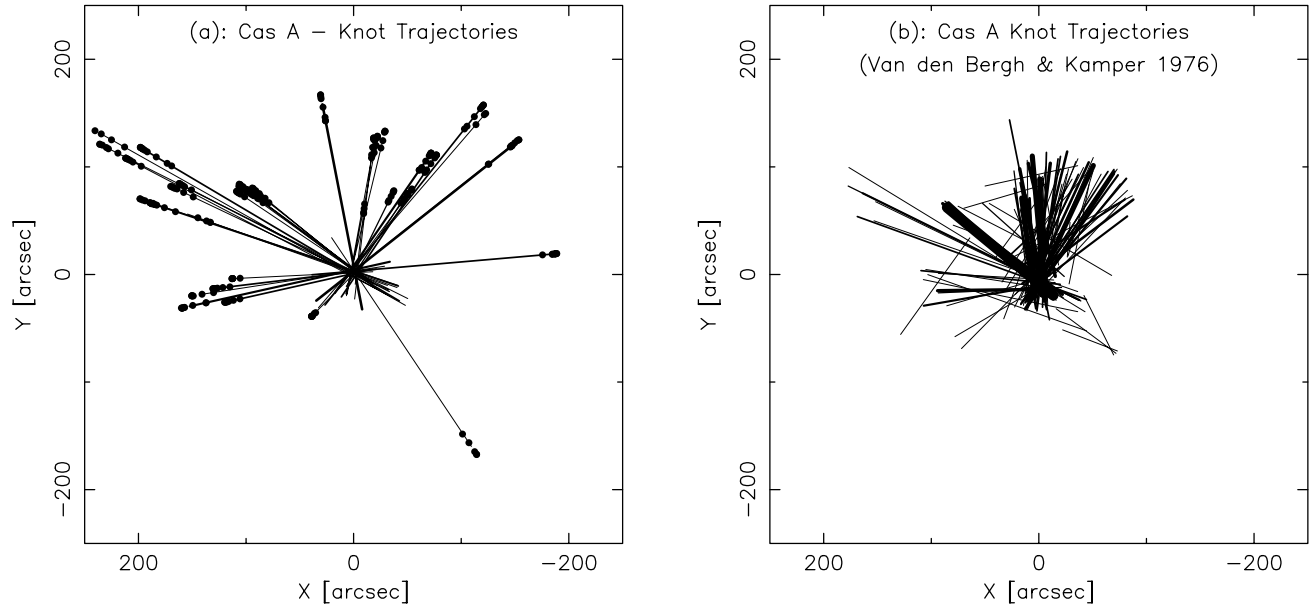

FIG. 2.—(*a*) Trajectories of the knots used in this study. The dots are individual measurements, and the lines are fits to the trajectories. The widths of the lines increase according to the weight in the solution. (*b*) Trajectories of the 102 knots used by Kamper & van den Bergh (1976).

TABLE 4

AGE AND CENTER OF EXPANSION MEASUREMENTS FOR CAS A

REFERENCE	SNR REGION	T_0 OR SNR AGE	EXPANSION CENTER COORDINATES	
			α(J2000)	δ(J2000)
Optical				
van den Bergh & Dodd 1970	Brt. shell	A.D. 1667 ± 8	23 23 27.16 ± 0.2	58 48 47.6 ± 3.1
Kamper & van den Bergh 1976	Brt. shell	A.D. 1653 ± 3	23 23 27.76 ± 0.1	58 48 46.7 ± 0.8
	NE jet	A.D. 1671 ± 3		
van den Bergh & Kamper 1983	Whole SNR	A.D. 1658 ± 3	23 23 27.76 ± 0.1	58 48 46.4 ± 1.0
Fesen, Becker, & Goodrich 1988	Outer knots	A.D. 1680 ± 15		
Kamper & van den Bergh 1991	Outer knots	A.D. 1671 ± 3		
Reed et al. 1995	Brt. shell		23 23 26.55 ± 0.09	58 49 00.7 ± 0.8
This paper	Outer knots	A.D. 1671.3 ±0.9	23 23 27.84 ± 0.06	58 48 49.4 ± 0.4
	Shell knots	A.D. 1662.3 ±1.7	23 23 27.71 ± 0.09	58 48 49.5 ± 0.7
	Whole sample	A.D. 1669.1 ±0.8	23 23 27.77 ± 0.05	58 48 49.4 ± 0.4
Radio				
Tuffs 1986	Brt. shell	Age = 949 yr	23 23 25.95 ± 0.4	58 48 48.4 ± 4.4
Green 1988	Brt. shell	Age ~ 400 yr		
Anderson & Rudnick 1995	Brt. shell	Age ~ 940 yr	23 23 26.05 ± 0.2	58 48 54.3 ± 3.1
	Outer knots	Age = 550–900 yr		
Agüeros & Green 1999	Brt. shell	Age = 400–500 yr		
X-Ray				
Vink et al. 1998	Brt. shell	Age = 501 ±15 yr		
Koralesky et al. 1998	Brt. shell	Age ~ 500 yr		

NOTE.—Units of right ascension are hours, minutes, and seconds, and units of declination are degrees, arcminutes, and arcseconds.

motion for each knot, which extrapolated back exactly to the observed maximum-likelihood position. We next created 1000 artificial data sets by adding Gaussian random noise to the idealized proper motions. For each artificial data set, we computed the maximum-likelihood center and its associated maximum λ.

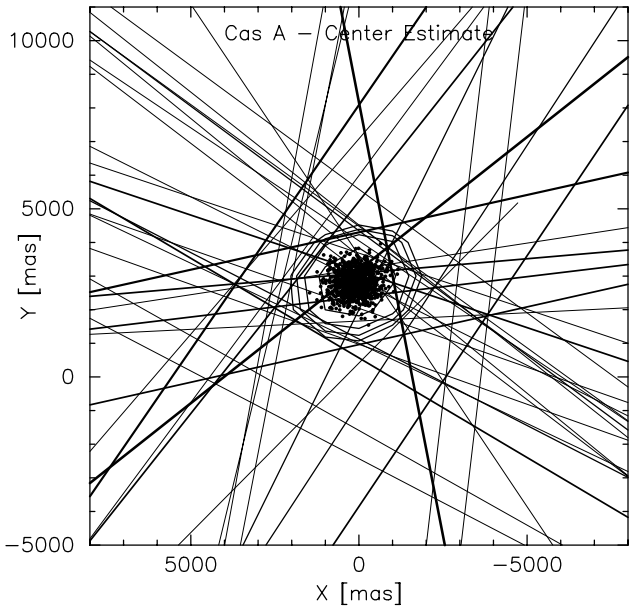

FIG. 3.—Magnified view of the region in which the knot trajectories intersect. The straight lines are the fitted trajectories, again with the line weight indicating the statistical weight. The contours represent confidence intervals for the centroid based on the likelihood ratio test, and represent 95% to 99.5% confidence. The dots are centroids determined from Monte Carlo simulations of the measurement. A "fudge factor" of 0.7 has been applied to the estimated errors for this calculation (see text). The origin of this plot is the KvdB76 estimate of the center of expansion; note the significant offset of the new determination from this position.

In the first trials, the standard deviation used for the Gaussian noise was simply the estimated proper motion uncertainty of each knot—in effect, we took our estimated position errors to be realistic. For nearly all the trials, this choice led to maximum values of λ larger than observed, indicating that the errors in the proper motions were overestimated (as expected since our error estimates were believed conservative). In the final Monte Carlo calculation, we multiplied the proper motion standard deviations by a global "fudge factor" $f \sim 0.7$.

These simulated data sets yielded maximum values of $\lambda(X, Y)$ very similar to that of the real data. The spread in the positions generated by this procedure should be a realistic indicator of the uncertainty in the centroid. The cloud of Monte Carlo positions is also shown in Figure 3 and has standard deviations in X and Y of 398 and 366 mas, respectively. Half of the points lie within 448 mas of the mean position and 95% within 946 mas. This agrees well with the likelihood-ratio test described above once the scaling factor of 0.7 is taken into account and provides a cross-check on the likelihood-ratio procedure.

As an additional check, we divided our data into two samples—shell knots and outer knots. The outer knots gave $X = 599$ mas, $Y = 2809$ mas with half the Monte Carlo points within 508 mas of the mean; the shell knots gave $X = -388$ mas and $Y = 2840$ mas, with half within 783 mas. The disagreements between these and the combined data are about as expected given the estimated statistical errors.

In a final statistical experiment we repeatedly selected half the knots at random found the maximum likelihood center of the subsample. For this we used the observed

trajectories without adding artificial noise. The distribution of the centers produced by 1000 such trials was rather elongated east-west ($\sigma_X = 666$ mas, $\sigma_Y = 410$ mas) but did not extend toward a particular direction (e.g., the KvdB76 and vdBK83 center). This shows that our center determination is not thrown off by a few stray knots.

4.1.2. *Comparison to Previous Results*

Previous center of expansion values from optical and radio data are listed in Table 4. The first accurate estimate of Cas A's expansion point was made by van den Bergh & Dodd (1970) using Palomar 5 m PF plates of 27 "fast-moving knots" covering the time period 1951 through 1969. KvdB76 later updated this to include a total of 102 knots covering the additional period 1970–1975. This study itself was supplemented by 1976–1980 measurements of 46 especially long-lived knots by vdBK83. The last two studies reached essentially the same central position estimate within measurement errors. More recently, Reed et al. (1995) found a significantly different expansion point based on a least-squares spherical fit to a plot of main shell knot radial velocities. However, this displaced center reflects radial velocity differences between back and front hemispheres and is thus unlikely to be an accurate measure of the remnant's expansion center.

Our estimated center lies only 3″ due north of the center derived by KvdB76 and vdBK83, but this is well outside their ±0.″8–1.″0 estimated uncertainty. Although our study includes far fewer knots (38) than they used, our results have smaller formal errors and the trajectories have a smaller dispersion. For comparison we show in Figure 2*b* trajectories of the 102 knots measured in the KvdB76 study at the same scale as the trajectories in Figure 2*a*. The larger spread in knot trajectories in the KvdB76 data largely reflects inclusion of fewer outlying knots and more main shell knots in their study.

Finally, we note that the two reported centers derived from radio measurements lie significantly (~15″) east of the centers estimated from the optical knots. Because the remnant's radio emission does not exhibit a smooth, globally coherent radial expansion (Bell 1977; Tuffs 1986; Anderson & Rudnick 1995), we believe that radio-derived centers are less meaningful.

4.1.3. *X-Ray Point Source*

First-light *Chandra* observations of Cas A revealed the presence of a pointlike X-ray source near the center (Tananbaum 1999). The source was subsequently confirmed through inspection of archival *ROSAT* (Aschenbach 1999) and *Einstein* data (Pavlov & Zavlin 1999). The X-ray source's position has been refined slightly using further *Chandra* observations (Murray et al. 2001, in preparation; Kaplan, Kulkarni, & Murray 2001). Table 5 lists this refined *Chandra* position, together with those estimated from investigations of *ROSAT* and *Einstein* HRI data. Figure 4 shows the *Chandra* position, and both KvdB76's and our expansion centers superposed on an optical image of the central region.

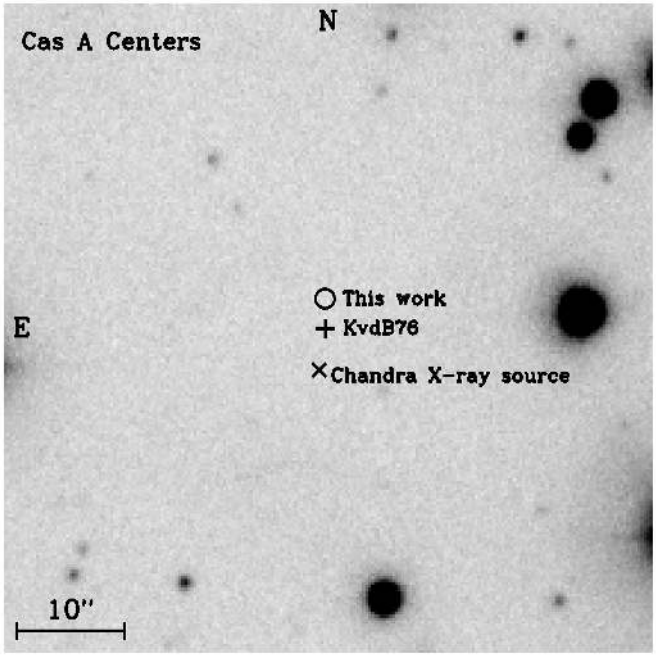

FIG. 4.—Image of the center of the Cas A supernova remnant taken with the MDM 2.4 m Hiltner telescope and a [S II] λλ6716, 6731 filter in 1″ seeing. The positions of the Chandra X-ray point source, the KvdB76 expansion center, and our revised expansion center are indicated.

The *Chandra* X-ray point source lies some 6.″6 south (position angle ≃354°) of our derived center of expansion for Cas A. Our new expansion center actually lies *farther away* from the *Chandra* position than does the KvdB76 center. Both the *ROSAT* and *Einstein* observations, however, place the X-ray point source a few arcseconds farther to the west and north, thus closer to our expansion center. Assuming a common origin for the ejecta knots and the point source, our center and the *Chandra* position together imply a transverse velocity of ≃330 km s^{-1} at a distance of 3.4 kpc. This velocity is not unusual for a young

TABLE 5

DERIVED CENTER OF EXPANSION VERSUS X-RAY POINT SOURCE

OBJECT	REFERENCE	COORDINATES	
		α(J2000)	δ(J2000)
Center of expansion	This paper	23 23 27.77 ± 0.05	58 48 49.4 ± 0.4
X-ray point source	*Chandra* ACIS[a]	23 23 27.86 ± 0.13	58 48 42.8 ± 1.0
X-ray point source	*ROSAT* HRI[b]	23 23 27.57 ± 0.75	58 48 44.0 ± 6.0
X-ray point source	*Einstein* HRI[b]	23 23 27.83 ± 0.50	58 48 43.9 ± 4.0
X-ray point source	*Einstein* HRI[b]	23 23 27.89 ± 0.50	58 48 43.7 ± 4.0

NOTE.—Units of right ascension are hours, minutes, and seconds, and units of declination are degrees, arcminutes, and arcseconds.

[a] Tananbaum 1999; Kaplan, Kulkarni, & Murray 2001; Murray et al. 2001, in preparation.

[b] From Pavlov et al. 2000.

pulsar, if this is indeed what it is (Umeda et al. 2000; Chakrabarty et al. 2001; McLaughlin et al. 2001).

4.2. *Explosion Date and Knot Deceleration*

Limits on the date of the Cas A SN explosion bear on two questions. First, could Flamsteed have seen it in A.D. 1680? Second, how much have the knots decelerated over the last 300 yr?

The outer and shell knot trajectories give significantly different ages, in the sense expected if the shell knots have decelerated more than the outer knots due to their interaction with a reverse shock. This trend is clearly visible in Figure 5, which shows the times at which the individual knots are computed to have passed closest to the center (assuming no deceleration); we will refer to this quantity as the *crossing time*. (Note: The center position used to compute the crossing times is derived from the whole data set. The knots move quickly enough that small variations in the placement of the center do not affect the trend.)

Because of their smaller deceleration, the outer knots offer a better estimate of the date of the Cas A supernova than ejecta in the bright shell. A straight average of the 17 outer knots' crossing times yields an explosion date of 1671.3 ± 0.9, while the 21 main shell knots yield 1662 ± 1.7. On the face of it, the outer knot data indicate a date 9 years earlier than Flamsteed's 1680 sighting of 3 Cas. However, a deceleration of only ~ 0.1 mas yr^{-2} for the outer knots would change the date by ~ 10 years. In our best-observed knots the 1 σ uncertainty in the deceleration approaches this value, but none of the knots show significant deceleration. There is also no trend for the fitted acceleration vectors to be pointed inward toward the center. Thus, we can neither directly detect nor disprove decelerations large enough to make Flamsteed's A.D. 1680 sighting coincide with the explosion.

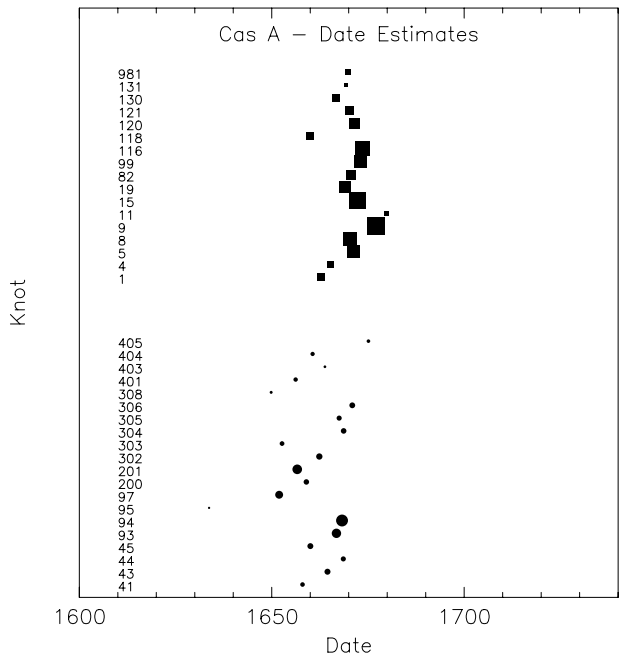

FIG. 5.—Dates at which the extrapolated knot trajectories pass nearest to the maximum likelihood center. The size of the symbol is inversely proportional to the estimated uncertainty. Outer knots (*squares*) are toward the top, and shell knots (*circles*) toward the bottom. Note the retardation and increased scatter of the shell.

The dispersion in the knots' crossing times also affects the case for Flamsteed's 1680 sighting. As noted above, the mean crossing time is displaced from 1680. If in addition the dispersion in crossing times were small, then in order for Flamsteed to have seen the explosion the different knots would need to have suffered nearly identical decelerations. This would be unlikely given the typical inhomogeneity of the ISM. However, Figure 5 shows enough scatter in the crossing times that a Flamsteed sighting remains plausible.

If we assume for a moment that the explosion date really was 1680 and that the knots have decelerated uniformly ever since, we can then compute an implied deceleration for each knot. For the nine best shell knots (those with formal 1 σ crossing time uncertainties less than 5 years), these implied decelerations range from 0.04 mas yr^{-2} for knot 9 to 0.14 mas yr^{-2} for knot 120, with a mean of 0.10 mas yr^{-1}. At 3.4 kpc, 0.10 mas yr^{-1} corresponds to a transverse acceleration of only 1.6 km s^{-1} yr^{-1} or a velocity change of some 2%–5% over the age of the remnant.

Detecting velocity changes $\sim$1–2 km s^{-1} yr^{-1} in these faint, outer ejecta knots to test plausible explosion dates would be difficult, but perhaps not impossible. The sudden brightening of knot 19 along the remnant's western limb during the early 1970's (Fesen 2001) suggests it may be decelerating significantly at the present epoch. A direct measurements of a knot's present-day deceleration could, in principle, be used to explore the density of the interstellar or circumstellar medium around the remnant. But at present not enough is known about the knots' masses, dimensions, and structure to draw reliable conclusions about their environment from their decelerations.

4.3. *Explicitly Time-Dependent Estimates*

As a check on the center and explosion date estimates, we also estimated these quantities jointly. Using the fitted knot trajectories, we stepped through a range of dates t around the explosion. At each date, we computed the weighted mean position of the knots and then computed

$$S = \sum_i \left[\frac{d_i(t)}{\sigma_{i0}} \right]^2 ,$$

where $d_i(t)$ is the angular distance of knot i from the mean center at date t. The estimated explosion date is then $t_{\min}$, the date which minimizes S. The weighted mean position of the knots at $t_{\min}$ is an estimate of the explosion center. This procedure yielded $t = 1671.5$, $X = +723$ and $Y = +2362$ for the outer knots, $t = 1659.8$, $X = +585$ and $Y = +1623$ for the shell knots, and $t = 1669.8$, $X = +856$, and $Y = +2693$ for the entire sample of knots. Because the knots in our sample are distributed nonuniformly around the remnant's periphery, differences in date translate into differences in position in a complicated way. The likely differential deceleration of the knots therefore makes this estimate less reliable than the previous estimate, which is based on lines of position. Nonetheless, the results are broadly similar—all the estimates put the best center significantly north of KvdB76's center, and the shell knots show evidence of deceleration.

5. CONCLUSIONS

Our new proper motions of 21 main-shell and 17 higher velocity, outer ejecta knots in Cas A leads to improved estimates of the center of expansion and the age. We find the

expansion center to be $\alpha(\mathrm{J2000}) = 23^{\mathrm{h}}23^{\mathrm{m}}27^{\mathrm{s}}.77 \pm 0^{\mathrm{s}}.05$, $\delta(\mathrm{J2000}) = 58^{\circ}48'49''.4 \pm 0''.4$, with little difference between the centers derived using outer or main shell knots. This expansion point lies $6''.6 \pm 1''.5$ to the north of the recently recognized X-ray point source. If the point source originated in the explosion, the position offset implies a transverse velocity of $\simeq 330$ km s^{-1} at a distance of 3.4 kpc.

Using the outer knots, most of which are in front of the main blast wave, we estimate a date of explosion of 1671.3 ± 0.9 assuming no deceleration. However, interaction with local CSM/ISM should decelerate the knots. If the velocities have declined by only a few percent over the age of the remnant, the remnant age would be consistent with a suspected sighting of the supernova by J. Flamsteed in 1680. The age derived from the main shell knots is greater by 9 yr than that derived from the outer knots, implying a greater deceleration of the main shell.

We are grateful to R. Barr and the MDM staff for their excellent assistance in instrument setup and preparation, to the Dunlap Observatory at the University of Toronto for shipment of several Palomar PF plates, and to C. Gerardy with assistance with *HST* image data reduction. Special thanks go to Terry Girard and John Lee at Yale for their generous assistance with the plate scanning, and to the Yale department for their hospitality. One of us (S. v. d. B.) would like to thank the Mount Wilson and Palomar Observatories for their kind hospitality, and generous allocation of significant amounts of 200 inch observing time over more than two decades that were used to observe the motions in Cassiopeia A. Van den Bergh would also like to thank the late Karl Kamper for many years of fruitful collaboration on the study of proper motions and brightness variations of the knots in Cas A. Partial support for this work was provided by NASA through grant number GO-7405-01A from the Space Telescope Science Institute, which is operated by AURA, Inc., under NASA contract NAS5-26555. J. R. T. thanks the NSF for support through grant number 9987334.

REFERENCES

Agüeros, M. A., & Green, D. A. 1999, MNRAS, 305, 957
Anderson, M. C., & Rudnick, L. 1995, ApJ, 441, 307
Aschenbach, B. 1999, IAU Circ. 7249
Ashworth, W. B. 1980, J. Hist. Astron., 11, 1
Bell, A. R. 1977, MNRAS, 179, 573
Bertin, E., & Arnouts, S. 1996, A&AS, 117, 393
Broughton, R. P. 1979, JRASC, 73, 381
Cash, W. 1979, ApJ, 228, 939
Chakrabarty, D., Pivovaroff, M. J., Hernquist, L. E., Heyl, J. S., & Narayan, R. 2001, ApJ, 548, 800
Cudworth, K. M., & Rees, R. F. 1991, PASP, 103, 470
Fesen, R. A. 2001, ApJS, 133, 161
Fesen, R. A., & Becker, R. H. 1991, ApJ, 371, 621
Fesen, R. A., Becker, R. H., & Blair, W. P. 1987, ApJ, 313, 378
Fesen, R. A., Becker, R. H., & Goodrich, R. 1988, ApJ, 329, L89
Fesen, R. A., & Gunderson, K. S. 1996, ApJ, 470, 967
Green, D. A. 1988, in Supernova Remnants and the Interstellar Medium, ed. R. S. Roger & T. L. Landecker (Cambridge: Cambridge Univ. Press), 51
Høg, E., et al. 2000, A&A, 355, L57
Holtzman, J., et al. 1995, PASP, 107, 156
Hughes, D. W. 1980, Nature, 285, 132
Kamper, K. W. 1980, Observatory, 100, 3
Kamper, K., & van den Bergh, S. 1976, ApJS, 32, 351 (KvdB76)
———. 1991, BAAS, 23, 821
Kaplan, D. L., Kulkarni, S. R., & Murray, S. S. 2001, preprint (astro-ph 0102054)
Koralesky, B., Rudnick, L., Gotthelf, E. V., & Keohane, J. W. 1998, ApJ, 505, L27
McLaughlin, M. A., Cordes, J. M., Deshpande, A. A., Gaensler, B. M., Hankins, T. H., Kaspi, V. M., & Kern, J. S. 2001, preprint (astro-ph/0010338)
Monet, D., et al. 1996, USNO-SA2.0 (Washington: US Naval Obs.)
Murray, C. A. 1971, MNRAS, 154, 429
Pavlov, G. G., & Zavlin, V. E. 1999, IAU Circ. 7270
Pavlov, G. G., Zavlin, V. E., Aschenback, B., Trümper, J., & Sanwal, D. 2000, ApJ, 531, L53
Reed, J. E., Hester, J. J., Fabian, A. C., & Winkler, P. F. 1995, ApJ, 440, 706
Ryle, M., & Smith, F. G. 1948, Nature, 162, 462
Stetson, P. B. 1987, PASP, 99, 191
Stone, R. C., Pier, J. R., & Monet, D. G. 1999, AJ, 118, 2488
Tananbaum, H. 1999, IAU Circ. 7246
Tuffs, R. J. 1986, MNRAS, 219, 13
Umeda, H., Nomoto, K., Tsuruta, S., & Mineshige, S. 2000, ApJ, 534, L193
van den Bergh, S., & Dodd, W. W. 1970, ApJ, 162, 485
van den Bergh, S., & Kamper, K. 1983, ApJ, 268, 129 (vdBK83)
———. 1985, ApJ, 293, 537
van den Bergh, S., & Pritchet, C. J. 1986, ApJ, 307, 723
Vink, J., Bloemen, H., Kaastra, J. S., Bleeker, J. A. M. 1998, A&A, 339, 201